Nuclear Instruments and Methods in Physics Research B 287 (2012) 60–67

Contents lists available at SciVerse ScienceDirect

Nuclear Instruments and Methods in Physics Research B

journal homepage: www.elsevier.com/locate/nimb

# Modifications of the registration properties of charged particles in a CR-39 polymeric track detector induced by thermal annealing

A.F. Saad *,[1], N.A. Hamed, Y.K. Abdalla, D.M. Tawati

*Physics Department, Faculty of Science, University of Benghazi, Benghazi, Libya*

ARTICLE INFO

*Article history:*
Received 24 May 2012
Received in revised form 4 July 2012
Available online 16 July 2012

*Keywords:*
Thermal annealing
Registration properties
Charged particles
Exposure pre- and post-annealing
Activation energy
CR-39 detectors

ABSTRACT

The thermal annealing behavior of alpha and fission fragment tracks, following exposure pre- and post-annealing, in a high polymer material of poly allyl diglycol carbonate (PADC), a form of CR-39, has been investigated as a function of temperature and time. Isothermal and isochronal annealing experiments were carried out on CR-39 polymeric detectors exposed to a $^{252}$Cf source. The yields of fission fragment and surviving alpha tracks were measured as a function of annealing time and temperature, as was the variation of fission track diameter with annealing time. The bulk and track etch rates were measured using alpha and fission fragment track diameters and the bulk etch rate was also measured by the weight loss method. The activation energy of annealing was determined using two different models based on the experimental results. This paper presents novel information showing that the annealed CR-39 detectors were demonstrated to be highly sensitive to the fission fragments, but not to alpha particles.



## 1. Introduction

Solid state nuclear track detectors (SSNTDs) have been studied over the last three decades in a wide range of different areas of science and technology, such as nuclear and high energy physics, cosmic-ray and astrophysics, material sciences, micro- and nanotechnology and many other fields [1–5]. These detectors are affected by many factors, such as temperature [6,7], pressure [8] and vacuum [9]. Temperature is the most important parameter affecting SSNTDs. At high temperature, the material used for polymeric detectors shows a significant increase in the rate of diffusion, which may cause significant disorder in the spacing between the constituent molecules of these detectors. Consequently, the effects of thermal annealing on nuclear tracks in solids have already been studied by several research groups [10–15]. An approach to the track formation mechanism and registration properties of charged particles in CR-39 SSNTDs, which can be understood, is a result of this annealing process [10,16–18]. A further consequence of this process is that heavy-ion tracks are more resistant to annealing than that those of lighter ions [19].

In the present work, we have studied the thermal annealing effect on the registration properties of alpha and fission fragments in a PADC polymeric material at temperatures ranging from 90 to 150 °C for rather long time intervals. For this purpose, several exposure experiments, with pre- and post-annealing of the CR-39 polymeric detector, were performed.

## 2. Annealing model

We used two annealing models as reported by Price et al. [7] and Mark et al. [20], to determine the activation energy of nuclear tracks in these SSNTDs. These two models of thermal annealing have been proposed to describe the annealing kinetics of nuclear tracks as a function of annealing time and temperature. The model by Price et al. [7] is given as follows:

$$\{[(S-1)_i-(S-1)_f]/(S-1)_i\} = At^{-n}\exp(-E_a/kT) \quad (1)$$

where $S = (V_T/V_B)$ and subscripts $i$ and $f$ refer to the initial and final values.

In this work, we also applied the annealing model introduced by Mark et al. [20] as follows:

$$\ln[-\ln D_0/D] = \ln\alpha_0 + \ln t - E_a/kT \quad (2)$$

where $D_0$ and $D$ are fission fragment track diameters at time $t = 0$ and $t$, respectively. $\alpha_0$ is the annealing constant and $k$ is the Boltzmann constant. Consequently, a plot of $\ln[-\ln D_0/D]$ against $10^3/T$ will produce a straight line of slope $E_a/k$.

## 3. Experimental procedure

For the present work, CR-39 detectors, having a thickness of 660 μm, were purchased from Intercast Europe S.P.A. of Parma,

* Corresponding author. Tel.: +218 92 8128608; fax: +218 61 2229617.
*E-mail address:* abdallahsaad56@hotmail.com (A.F. Saad).
[1] On leave from: Physics Department, Faculty of Science, Zagazig University, Zagazig, Egypt.

0168-583X/$ - see front matter © 2012 Elsevier B.V. All rights reserved.
http://dx.doi.org/10.1016/j.nimb.2012.07.005

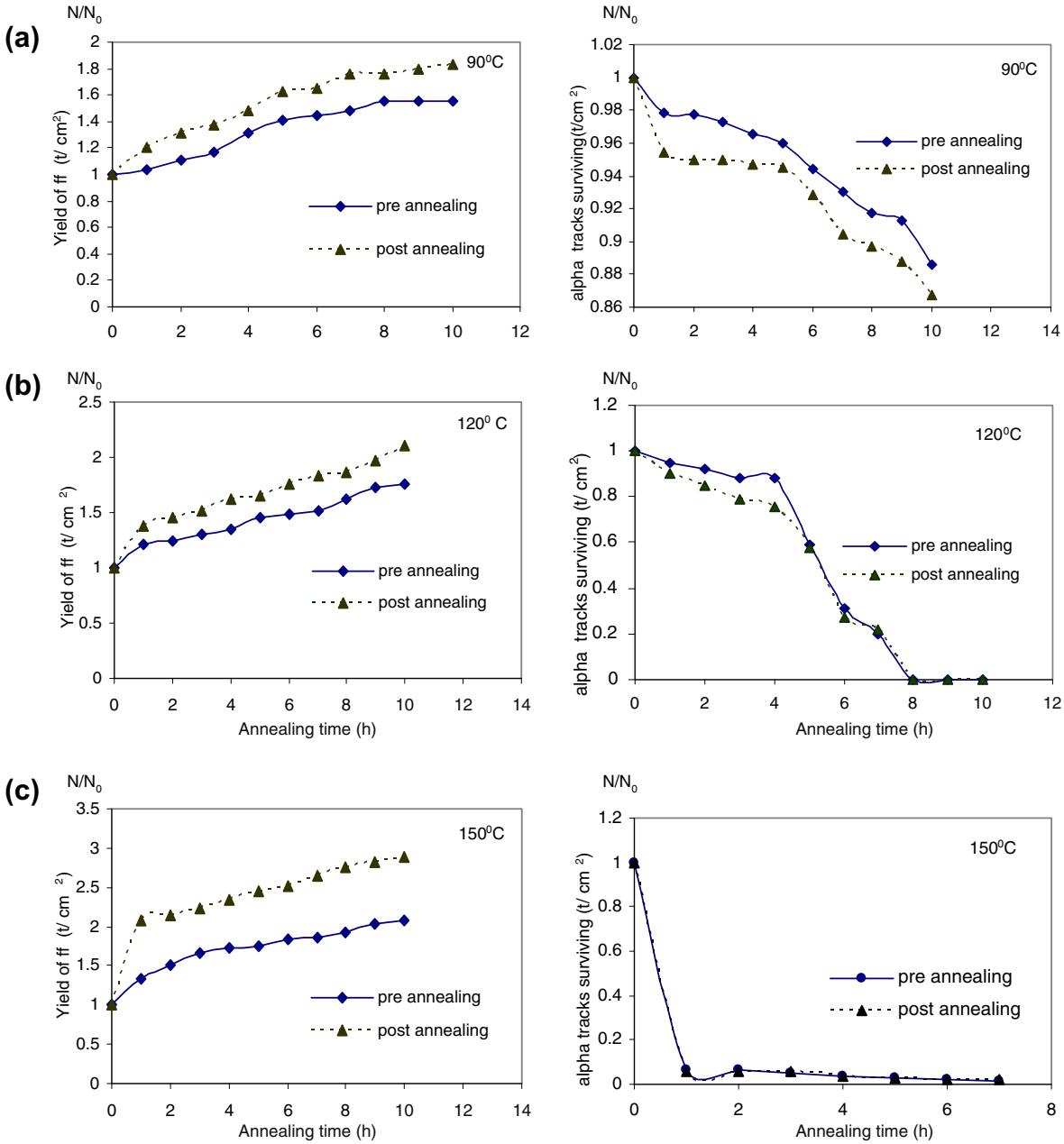


**Fig. 1.** The effect of isothermal annealing (exposure pre- and post-annealing) on the track density in a CR-39 plastic detector. The left hand side shows the variation of the yield of fission fragment tracks as a function of annealing time at three different temperatures; 90, 120 and 150 °C. The right hand side also shows the variation of the survival of alpha particle tracks as a function of annealing time at the same temperatures.

Italy. Three sets of detectors were prepared for this experiment, and all were irradiated with fission fragments and alpha particles from a $^{252}$Cf source. The irradiation was performed in air using $2\pi$ geometry. The irradiated detectors were then annealed in a temperature-controlled oven for different time intervals and at different temperatures. The first set of CR-39 detectors was exposed, but not annealed, in order to compare it with the results from annealed detectors (for the control experiments). The second set of detectors was first irradiated with fission fragments and alpha particles and then annealed in the oven (exposure pre-annealing). The third set was first annealed in the oven and then irradiated with fission fragments (exposure post-annealing).

After thermal treatment and irradiation or vice versa, the detectors were then etched in a 6.25 N standard aqueous solution of NaOH maintained at 70 °C by a water bath, which represents the most traditional etching conditions for CR-39 SSNTDs. The temperature was kept constant with a maximum uncertainty of ±1 °C. The etching time was chosen appropriately to ensure that the fission fragment tracks are reasonable observable using an optical microscope with appropriate magnification, but the alpha tracks have disappeared.

## 4. Results and discussion

The effect of annealing (isothermal and isochronal) in dry air on the α-particle and fission fragment track densities in both cases, exposure pre- and post-annealing, of the CR-39 plastic detectors is shown in Figs. 1 and 2. The density for α-particle and fission fragment tracks registered using annealed detectors has been

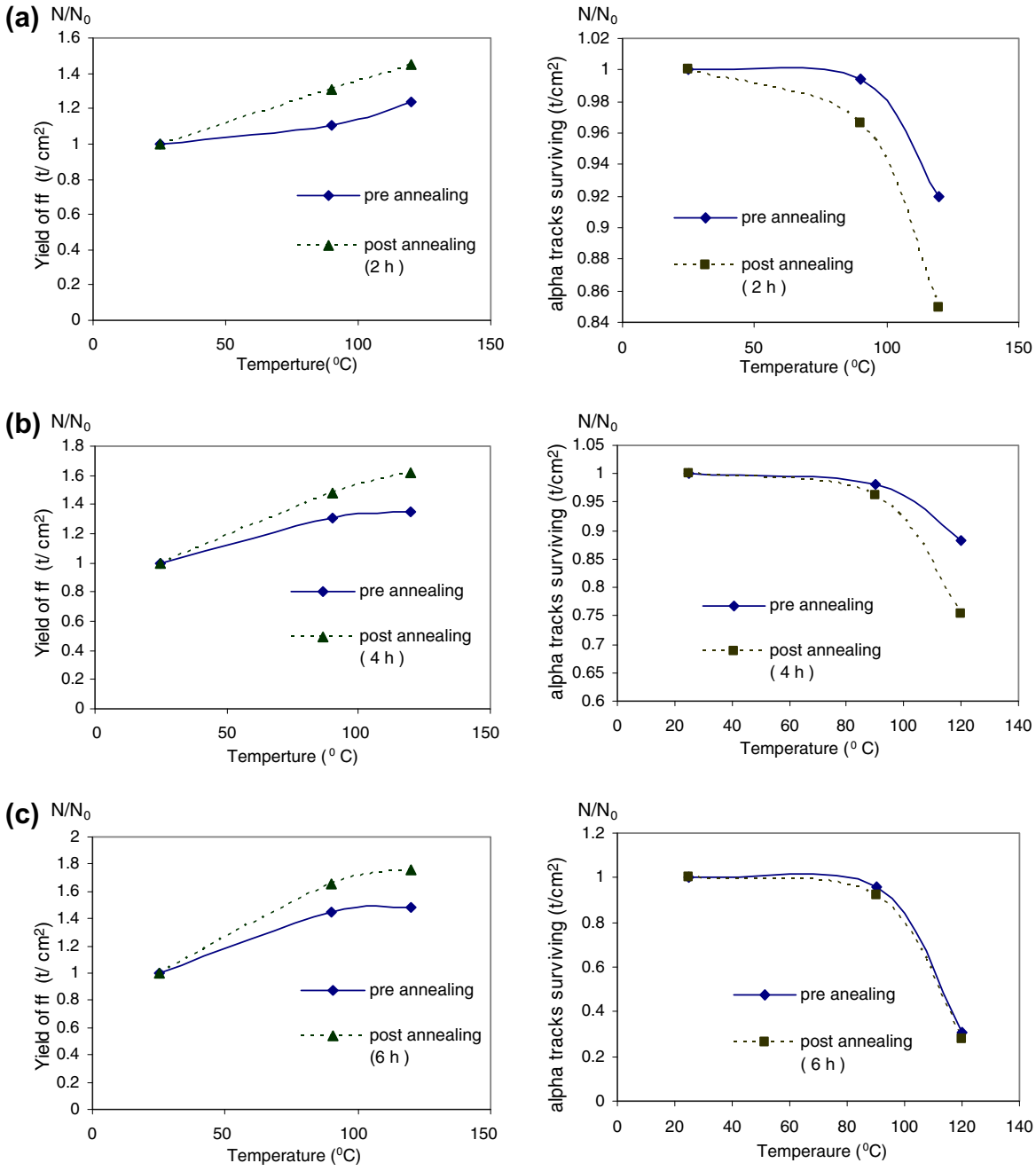


**Fig. 2.** The effect of isochronal annealing (exposure pre- and post-annealing) on the track density in a CR-39 plastic detector. The left hand side shows the variation of the yield of fission fragment tracks as a function of annealing temperature after (a) 2 h, (b) 4 h and (c) 6 h, respectively. The right hand side also shows the variation of the survival of alpha particle tracks as a function of annealing temperature at the same times.

normalized to an un-annealed one. In both figures, the α-particle track density exhibits the opposite behavior pattern of fission fragments. This means that the left hand side shows an increase in fission fragment track density while the right hand side shows a decrease in α-particle track density, until the α-particle tracks have more or less disappeared at higher temperatures. In addition, the fission fragment density in the case of exposure post-annealing is fairly high compared with exposure pre-annealing, while α-particles show the opposite effect.

In Fig. 1a (left hand side) the fission fragment track density increased non-linearly with annealing time at a temperature of 90 °C. Between 0 and 3 h there is a 12 and 25% increase in track density for exposure pre- and post-annealing, respectively. From 3 to 5 h there is a small sharp increase of 22 and 28% in track density, respectively. Beyond 5 h the track density slightly increases until 10 h for exposure post-annealing, while for exposure pre-annealing the track density slightly increases from 5 to 8 h, remaining constant thereafter. The right hand side of Fig. 1a shows that the α-particle track density decreased non-linearly with increased annealing time. After 1 h annealing, there is a decrease of 2 and 5% in track density for exposure pre- and post-annealing, respectively. From 1 to 5 h there is an insignificant decrease in track density, but a considerable decrease thereafter. In Fig. 1b, the left hand side also shows that at 1 h annealing there is a sharp increase of 25 and 40% in fission fragment track density for exposure pre- and post-annealing, respectively, and an additional increase of 30 and

**Table 1**
Values of etching and annealing parameters and diameter ratio of un-annealed and annealed fission fragment tracks $D_0/D$, $V_B$, $V_T$, $\eta\% = [1-(V_B/V_T)]$, $S = (V_T/V_B)$ and $\theta_c$ or annealing temperatures and times (exposure pre annealing) of CR-39 polymeric track detector.

| Annealing temperature (°C) | Annealing time (h) | Etching time (h) | $D_0/D$ | $V_B$[a] (μm/h) | $\eta\%$ | $V_T$ (μm/h) | S[b] | $\theta$[c] |
|---|---|---|---|---|---|---|---|---|
| Unannealed | 0 | 4 | – | 1.35 | 47.67 | 2.58 | 1.91 | 31.55 |
| 90 | 1 | 4 | 0.996 | 1.46 | 47.10 | 2.76 | 1.89 | 31.94 |
| | 2 | 4 | 0.984 | 1.53 | 46.88 | 2.88 | 1.88 | 31.10 |
| | 3 | 4 | 0.981 | 1.68 | 46.13 | 3.12 | 1.86 | 32.58 |
| | 4 | 4 | 0.972 | 1.77 | 45.87 | 3.27 | 1.85 | 32.77 |
| | 5 | 4 | 0.969 | 1.88 | 45.66 | 3.46 | 1.84 | 32.91 |
| | 6 | 4 | 0.967 | 1.93 | 45.01 | 3.51 | 1.82 | 33.36 |
| | 7 | 4 | 0.962 | 2.00 | 44.75 | 3.62 | 1.81 | 33.54 |
| | 8 | 4 | 0.960 | 2.08 | 43.48 | 3.68 | 1.77 | 34.42 |
| | 9 | 4 | 0.958 | 2.86 | 42.91 | 5.01 | 1.75 | 34.81 |
| | 10 | 4 | 0.954 | 3.62 | 41.89 | 6.23 | 1.72 | 35.53 |
| 120 | 1 | 4 | 0.957 | 1.68 | 35.14 | 2.59 | 1.54 | 40.44 |
| | 2 | 4 | 0.917 | 2.00 | 27.54 | 2.76 | 1.38 | 46.44 |
| | 3 | 4 | 0.761 | 2.44 | 25.38 | 3.27 | 1.34 | 48.26 |
| | 4 | 4 | 0.674 | 2.87 | 16.57 | 3.44 | 1.20 | 56.54 |
| | 5 | 4 | 0.497 | 3.66 | 17.38 | 4.43 | 1.21 | 55.71 |
| | 6 | 3 | 0.493 | 4.53 | 10.65 | 5.07 | 1.12 | 63.31 |
| | 7 | 2.5 | 0.465 | 5.35 | 5.15 | 5.83 | 1.09 | 66.59 |
| | 8 | 2.5 | 0.450 | 6.21 | 3.87 | 6.46 | 1.04 | 74.01 |
| | 9 | 2.25 | 0.443 | 8.43 | 2.88 | 8.68 | 1.03 | 76.22 |
| | 10 | 2.25 | 0.422 | 10.45 | 1.97 | 10.66 | 1.02 | 78.61 |
| 150[c] | 1 | 4 | 0.547 | – | – | – | 1.19 | 57.09 |
| | 2 | 4 | 0.520 | | | | 1.14 | 61.16 |
| | 3 | 4 | 0.510 | | | | 1.13 | 61.93 |
| | 4 | 4 | 0.465 | | | | 1.12 | 63.32 |
| | 5 | 4 | 0.457 | | | | 1.10 | 65.22 |
| | 6 | 4 | 0.453 | | | | 1.06 | 70.73 |
| | 7 | 4 | 0.443 | | | | 1.04 | 74.36 |
| | 8 | 4 | 0.437 | | | | 1.03 | 76.54 |
| | 9 | 4 | 0.434 | | | | 1.02 | 78.61 |
| | 10 | 4 | 0.431 | | | | 1.01 | 82.79 |

[a] $V_b$ was determined by weight loss method.
[b] S was determined by fission fragments (ff) method.
[c] For 150 °C: etching time in minutes and $V_b$ and $V_t$ was measured in μm/min.

60% from 1 to 10 h. It should be noted that, over the whole annealing time, there is over a 100% increase in track density in the case of exposure post annealing, but a lesser increase in track density for pre-annealing exposure. The right hand side of Fig. 1b also shows that from 0 to 4 h there is a decrease of 10 and 25% in the α-particle track density for exposure pre- and post-annealing, respectively. From 4 to 8 h there is a sharp decrease of about 80% in the track density and beyond 8 h the α-particle tracks completely disappear up to 10 h. In Fig. 1c the left hand side shows that at 1 h annealing there is over a 100% increase for exposure post-annealing, while for exposure pre-annealing there is a far lesser increase in fission fragment track density. Beyond 1 h and up to 10 h the rate of increase of track density between exposure pre- and post-annealing is nearly constant. The right hand side of Fig. 1c shows that from 1 to 10 h no α-particle tracks have registered. Materials heated at 120 °C beyond 7 h and at 150 °C from 1 h up to 10 h indirectly show that heat alters the internal morphology of the polymer, as previously observed [21]. This experimental evidence may be attributed to a probable rearrangement of the polymer chain spacings, consequently changing the registration properties of the ionizing particles, α-particles and fission fragments, and fast neutrons. Other research groups have also observed the nature of the mechanisms that cause changes in the track etch parameters due to thermal treatment [22–26].

Fig. 2 shows the effect of isochronal annealing for 2, 4 and 6 h at 90, 120 and 150 °C on the track density of the fission fragments and α-particles for exposure pre- and post-annealing. Overall, the isochronal annealing process tends to increase the fission fragment track density and decrease the α-particle track density until they disappear at higher temperatures. The CR-39 polymer usually will have suffered serious degradation due to annealing at these temperatures. The surface material of CR-39 then becomes permanently softened, producing an increase in the bulk etch rate, which results in a decrease in the detection sensitivity and detection thresholds for both kinds of ionizing particles, as shown in Tables 1 and 2. It is quite clear that there is a considerable modification of the CR-39 material induced by the thermal treatment process in respect to the registration properties of heavy ions. This means that thermally treated CR-39 becomes rather sensitive to heavily ionizing particles e.g. fission fragments, compared with particles with lower ionization rate, e.g. α-particles. Photomicrographs of etch pits due to alpha particles and fission fragments incident on un-annealed and annealed, exposure pre- and post-annealing, CR-39 samples at 120 °C for annealing duration periods of 0, 4, 8 and 10 h, respectively, are shown in Figs. 3 and 4.

Tables 1 and 2 show the effect of annealing (exposure pre- and post-annealing) on the diameter of the fission tracks $D_{ff}$, the bulk and track etch rates $V_B$ and $V_T$, respectively, the detection efficiency $\eta\% = [1-(V_B/V_T)]$, the sensitivity $S$, critical angle $\theta_c$ and etching behavior of the CR-39 polymeric nuclear track detector. The sensitivity $S$, which in turn involves the bulk etch rate as well as the track etch rate, decreases as the annealing time increases. The bulk etch rate was found to have changed due to the annealing process [27] although this change is relatively small compared to the change of track etch rate at 90 °C. It is greater at 120 °C, while at higher temperature, such as 150 °C when etching times are extremely short and measured in minutes, the change in both etch rates is very small. The measurement of this tiny change in etch rates is very difficult so we have applied a relationship which does not involve $V_B$ but, nevertheless, fits the annealing data well [6].

**Table 2**
Values of etching and annealing parameters and diameter ratio of un-annealed and annealed fission fragment tracks $D_0/D_w$, $V_B$, $V_T$, $\eta\% = [1- (V_B/V_T)]$, $S = (V_T/V_B)$ and $\theta_c$ for annealing temperatures and times (exposure post annealing) of CR-39 polymeric track detector.

| Annealing temperature (°C) | Annealing time (h) | Etching time (h) | $D_0/D$ | $V_B$[a] (μm/h) | η% | $V_T$ (μm/h) | S[b] | $\theta$[c] |
|---|---|---|---|---|---|---|---|---|
| Unannealed | 0 | 4 | – | 1.35 | 47.67 | 2.58 | 1.91 | 31.55 |
| 90 | 1 | 4 | 0.998 | 1.46 | 47.29 | 2.77 | 1.90 | 31.81 |
| | 2 | 4 | 0.987 | 1.53 | 47.06 | 2.89 | 1.89 | 31.97 |
| | 3 | 4 | 0.985 | 1.68 | 46.84 | 3.16 | 1.88 | 32.12 |
| | 4 | 4 | 0.981 | 1.77 | 46.53 | 3.31 | 1.87 | 32.33 |
| | 5 | 4 | 0.980 | 1.88 | 46.13 | 3.49 | 1.86 | 32.59 |
| | 6 | 4 | 0.977 | 1.93 | 44.38 | 3.47 | 1.80 | 33.79 |
| | 7 | 4 | 0.974 | 2.00 | 44.44 | 3.60 | 1.80 | 33.75 |
| | 8 | 4 | 0.970 | 2.08 | 43.17 | 3.66 | 1.76 | 34.63 |
| | 9 | 4 | 0.966 | 2.86 | 42.80 | 5.00 | 1.75 | 34.89 |
| | 10 | 4 | 0.960 | 3.62 | 42.17 | 6.26 | 1.73 | 35.33 |
| 120 | 1 | 4 | 0.968 | 1.68 | 35.14 | 2.59 | 1.54 | 40.44 |
| | 2 | 4 | 0.918 | 2.00 | 34.21 | 3.04 | 1.52 | 41.14 |
| | 3 | 4 | 0.766 | 2.44 | 29.48 | 3.46 | 1.42 | 44.85 |
| | 4 | 4 | 0.674 | 2.87 | 27.53 | 3.96 | 1.38 | 46.45 |
| | 5 | 4 | 0.500 | 3.66 | 20.09 | 4.58 | 1.25 | 53.05 |
| | 6 | 3 | 0.497 | 4.53 | 10.65 | 5.07 | 1.20 | 63.23 |
| | 7 | 2.5 | 0.469 | 5.35 | 9.17 | 5.89 | 1.10 | 65.27 |
| | 8 | 2.5 | 0.458 | 6.21 | 4.75 | 6.52 | 1.05 | 75.26 |
| | 9 | 2.25 | 0.446 | 8.43 | 3.88 | 8.77 | 1.04 | 73.99 |
| | 10 | 2.25 | 0.426 | 10.45 | 2.88 | 10.76 | 1.03 | 76.21 |
| 150[c] | 1 | 4 | 0.554 | – | – | – | 1.20 | 56.02 |
| | 2 | 4 | 0.522 | | | | 1.17 | 58.88 |
| | 3 | 4 | 0.518 | | | | 1.15 | 60.12 |
| | 4 | 4 | 0.475 | | | | 1.14 | 61.32 |
| | 5 | 4 | 0.462 | | | | 1.13 | 60.20 |
| | 6 | 4 | 0.455 | | | | 1.08 | 67.53 |
| | 7 | 4 | 0.451 | | | | 1.04 | 74.36 |
| | 8 | 4 | 0.444 | | | | 1.03 | 76.54 |
| | 9 | 4 | 0.440 | | | | 1.02 | 78.61 |
| | 10 | 4 | 0.423 | | | | 1.01 | 82.79 |

[a] $V_b$ was determined by weight loss method.
[b] S was determined by fission fragments method.
[c] For 150 °C: etching time in minutes and $V_B$ and $V_t$ was measured in μm/min.

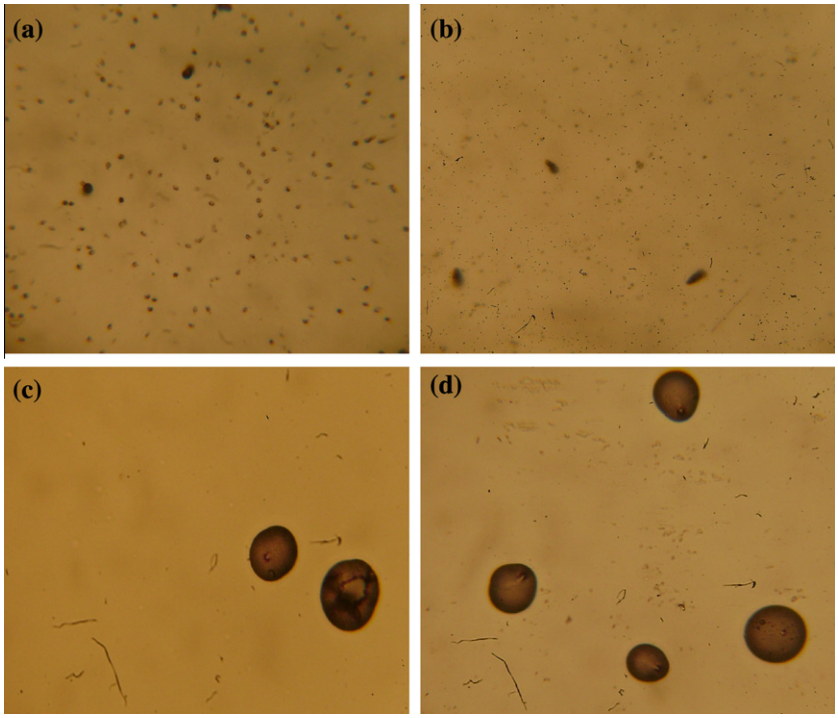


**Fig. 3.** Photomicrographs of annealed (exposure pre-annealing) of CR-39 detectors at temperature 120 °C for annealing periods of 0, 4, 8 and 10 h.

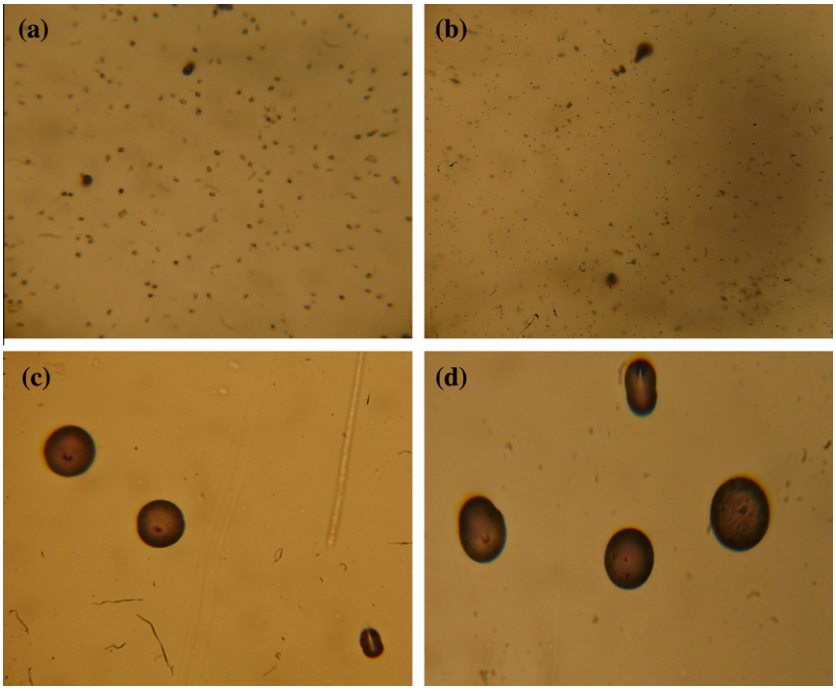


**Fig. 4.** Photomicrographs of un-annealed and annealed (exposure post-annealing) of CR-39 detectors at 120 °C for annealing periods of 0, 4, 8 and 10 h.

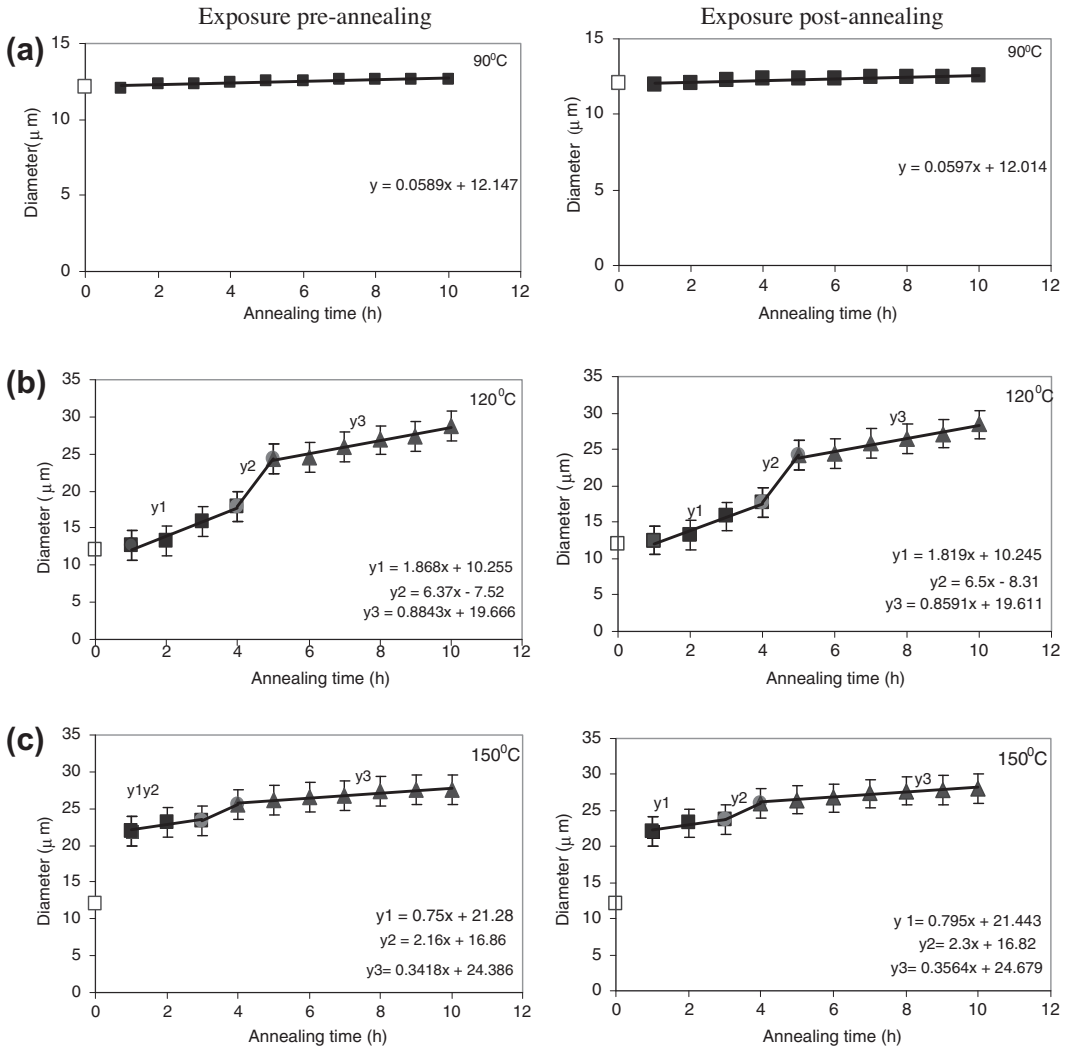


**Fig. 5.** Variation of fission fragment diameters as a function of annealing time at different temperatures.

We have plotted the mean track diameters of selected, large tracks of fission fragments along the minor axis in CR-39 SSNTDs as a function of annealing time at three different temperatures 90, 120 and 150 °C (for exposure pre- and post-annealing), as seen in Fig. 5. In general, the fission fragment track diameters increase with increasing annealing time and temperature, while the alpha track diameters generally show the opposite trend. The rate of increase depends strongly on the annealing temperature. At a temperature of 90 °C, there is a very small increase of track diameter with annealing time. For an annealing temperature 120 °C, the results show a different behavior where the variation of fission track diameter with annealing time has three different rates. As seen in Fig. 1b, the fission track diameter $D_{ff}$ increases linearly to 6 h. For an annealing time from 6 to 7 h, the rate of variation becomes fairly large and for a longer time, the rate becomes just a little greater than for the first stage. However, at 150 °C, the fission track diameter increases very sharply from 0 h (un-annealed) up to 1 h, but the rate of variation of $D_{ff}$ is somewhat smaller than that of sample annealed at 120 °C from 1 h until the end of the annealing time. In general, the annealing process is assumed to be a diffusion process in which displaced atoms are restored to their original positions, influenced by thermal energy. Once a heavy ion enters the detector material, the first tracks to be annealed are at the end and the etchable diameter increases from the beginning of the track. The density of extended defects is proportional to the energy deposited and, at the beginning of annealing process, the track tail is annealed where density of extended defects is not very large. As a result, annealing rate is high and is reduced with annealing time due to an increase in the density of extended defects in the upward direction of the damaged trail [6] and references therein. Our results show that the enhancement of track diameters become faster at lower annealing times and higher temperatures.

The most crucial parameter of the annealing process is the activation energy, which is an intrinsic property of the detector material. The effect of annealing on the activation energy of the CR-39 detector material has also been investigated. This crucial parameter has been determined based on the two important annealing models of Price et al. [7] and Mark et al. [20]. We have plotted $\ln\{[(S-1)_i-(S-1)_f]/(S-1)_i\}$ and $\ln[-\ln D_0/D]$ against $10^3/T$ for annealing times ranging from 1 to 4 h and these can be seen in Fig. 6. The data at longer annealing time, ranging from 5 to 10 h, was also plotted, but the scatter was too high, meaning that we need to apply a model involving two activation energies (high and low temperatures), and this will be the subject of a separate study. The values of activation energy, estimated from the slopes of straight lines fitted to our experimental data, are given in Table 3. The results show that the $E_a$ values decrease as the annealing time increases. Thus, we can say that our present study proves that the activation energies of annealing tracks in CR-39 is rather dependent on the annealing time. This is very consistent with published annealing data for $^{93}$Nb and $^{238}$U tracks [16], although these results show that the activation energy was reduced with annealing time, while it shows no dependence on annealing time in the case of CR-39 [28]. This may be because the annealing time intervals were not long enough whereas in the current study, the thermal annealing was so severe because the annealing times were long, ranging from 1 to 10 h.

**Table 3**
Values of activation energy $E_a$ at annealing temperatures of 90, 120 and 150 °C (isochronal annealing) as a function of annealing time, using the annealing track models of Price et al. [7] and Mark et al. [20].

| Annealing time (h) | Activation energy (eV) | |
|---|---|---|
| | Price et al. model | Mark et al. model |
| 1 | 0.88 | 1.10 |
| 2 | 0.80 | 0.81 |
| 3 | 0.68 | 0.79 |
| 4 | 0.64 | 0.74 |

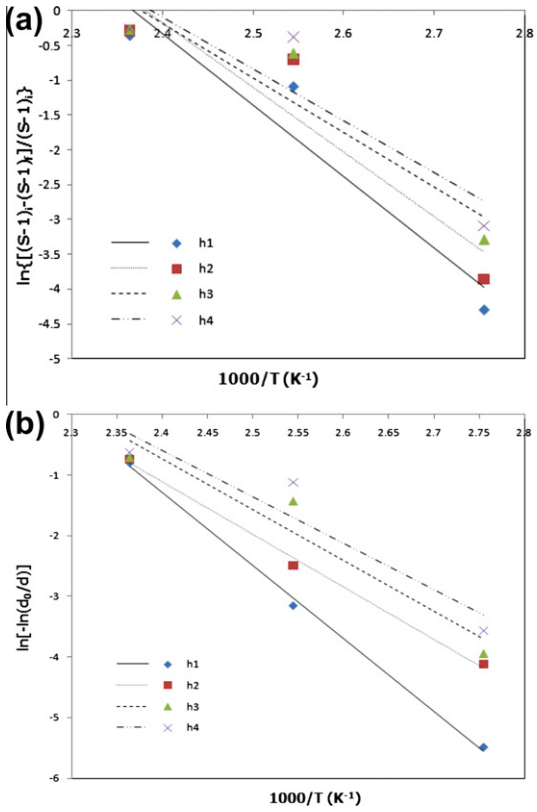


**Fig. 6.** Annealing results of $^{252}$Cf alpha particles and fission fragment tracks in CR-39 NTDs based on: (a) Price et al. [7], (b) Mark et al. [20].

## 5. Conclusions

- Thermal annealing induced significant modifications of the density and diameter of the alpha particle and fission fragment tracks in CR-39 plastic detectors.
- The detector material was demonstrated to be very sensitive to particles with higher ionizing rates, for example fission fragments, and not to ones with lower ionizing rates, such as alpha particles.
- The concept of a single activation energy provides a satisfactory explanation of the annealing process of nuclear tracks in a CR-39 polymeric detector for short annealing times, but for longer times we need to apply the concept of two activation energies, for high and low temperatures.
- The current results show that thermal annealing effects in CR-39 polymeric material play an important role in particle identification, especially in the high energy and nuclear physics fields.

## Acknowledgements

We would like to thank the Benghazi University's Zoology Department of the Faculty of Science for providing an optical microscope during the track scanning work and special thanks to Prof. Mahmoud Fadiel the Ex. Dean of our Faculty for his encouragement and assistance. We also acknowledge Mr. Mohammed El-Mshatay for his technical assistance.

## References


[1] P.B. Price, J.D. Stevenson, S.W. Barwick, Phys. Rev. Lett. 54 (1985) 297.
[2] M. Fujii, A.F. Saad, Y. Hatano, et al., Radiat. Meas. 34 (2001) 255.
[3] S.W. Barwick, P.B. Price, J.D. Stevenson, Phys. Rev. 31 (1985) 1985.
[4] A.F. Saad, S.T. Atwa, Y. Yokota, M. Fujii, Radiat. Meas. 40 (2005) 780.
[5] A.F. Saad, A.A. El-Namrouty, S. Solyman, S.T. Atwa, J. Korean Phys. Soc. 58 (2011) 701.
[6] M.A. Rana, I.E. Qureshi, E.U. Khan, et al., Nucl. Instr. Meth. Phys. Res. B 170 (2000) 149.
[7] P.B. Price, G. Gerbier, H.S. Park, M.H. Salamon, Nucl. Instr. Meth. Phys. Res. B 28 (1987) 53.
[8] J. Drach, M.H. Salamon, M. Solarz, P.B. Price, Nucl. Instr. Meth. Phys. Res. B 23 (1987) 367.
[9] M. Fujii, R. Yokota, T. Kobayashi, H. Hasegawa, Radiat. Meas. 28 (1997) 61.
[10] R.L. Fleischer, P.B. Price, E.M. Symes, D.S. Miller, Science 143 (1964) 349.
[11] G. Hussain, H.A. Khan, Radiat. Eff. 29 (1976) 53.
[12] N.A. Karamoust, S.A. Durrani, Nucl. Tracks Radiat. Meas. 19 (1991) 179.
[13] S. Anupam, Kumar, Radiat. Meas. 28 (1997) 181.
[14] R.K. Jain, G.S. Rhandhawa, S.K. Rose, H.S. Virk, J. Phys. D Appl. Phys. 31 (1998) 328.
[15] T. Sawamura, B. Satoshi, M. Narita, Radiat. Meas. 30 (1999) 453.
[16] H.S. Virk, S.K. Modgil, R.K. Bhatia, Nucl. Tracks Radiat. Meas. 11 (1986) 323.
[17] R.K. Bhatia, R.C. Singh, H.S. Virk, Nucl. Instr. Meth. Phys. Res. B 46 (1990) 358.
[18] S.A. Durrani, N.A. Karamoust, I.J.M. Al-Khalifa, Radiat. Prot. Dosim. 34 (1990) 43.
[19] M. Maurette, Radiat Eff 5 (1970) 15.
[20] T.D. Mark, R. Vartanian, F. Purtscheller, M. Pahl, Acta Phys. 53 (1981) 45.
[21] A. Aframian, Radiat. Phys. Chem. 12 (1978) 63.
[22] C.F. Wong, D.W. Field, Radiat Eff 81 (1984) 31.
[23] A.A. Abou El-Khier, M. Gaber, S.A. Mahmoud, E. El-Shafey, Mater. Lett. 24 (1995) 41.
[24] N.E. Ipe, P.L. Ziemer, Nucl. Tracks Radiat. Meas. 11 (1986) 137.
[25] M.A. Rana, Nucl. Instr. Meth. Phys. Res. A 672 (2012) 57.
[26] R.K. Jain, A. Kumar, B.K. Singh, Nucl. Instr. Meth. Phys. Res. B 274 (2012) 100.
[27] M.H. Salamon, P.B. Price, J. Drach, Nucl. Instr. Meth. Phys. Res. B 17 (1986) 173.
[28] M.A. Rana, I.E. Qureshi, S. Manzoor, et al., Nucl. Instr. Meth. Phys. Res. B 179 (2001) 179.